

Effects of Pipes Corrugated Shapes on the Friction Factor

Ismail O.S. ** and Tairu O.O.*

*Author for correspondence

Department of Mechanical Engineering,
Yaba College of Technology, yaba Nigeria.

Email: onatairu@gmail.com

**University of Ibadan, Ibadan, Nigeria

ABSTRACT

Corrugated pipes are pipes with walls of rough surfaces consisting of discrete grooves periodically disposed along the flow direction and commonly use in engineering application such as irrigation, delivery devices to main distribution ducts as in transport of Liquid Natural Gas from ships to the mainland distribution network and heat exchanger in heating, ventilation, air-conditioning etc. The simulation of turbulent, incompressible, isothermal and single-phase flow is considered for five geometric configurations of corrugated surfaces with the different groove heights, length and spacing were evaluated in order to compare their influence on the friction factor. The numerical analysis was carried out using computational fluid dynamics, and the two-equation turbulence models was used to compute the friction factors and Reynolds number for comparison. The results shows that the friction factor is not solely depend on the roughness height but also on the thickness of the roughness and space between successive roughness.

INTRODUCTION:

Corrugated pipes are pipes use in various engineering application such as irrigation, transportation of Liquid Natural Gas from ships, and as heat exchanger in heating, ventilation, air-conditioning etc with walls of rough surfaces groove periodically along the flow direction. They are also used as culverts at road crossings in Canada, the United States, and other countries, as velocities reduction in the culverts for fish to travel upstream. Since the pipes are large use in many engineering device, the effect of the corrugated surfaces on the flow properties have been in study for many years. The flow in a pipe or the flow between moving parallel plates (plane Couette flow) behave different ways and various studies on the flow of fluid in pipes have be in consideration in past and have helped to advance both our understanding of the various

transition scenarios and of the properties of fluid. The main features of turbulence transition in a pipe were documented long ago by Reynolds [1]. He noticed the possibility to delay the transition by suppressing perturbations in the inflow region, the intermittent character of the transition, and the presence of vortices in the turbulent regions. He noticed that the flow can be characterized by a dimensionless combination of mean downstream velocity U , radius of the pipe R and kinematic viscosity ν , nowadays known as the Reynolds number $Re = 2UR/\nu$. The intermittent character of the transition and absence of a linear instability of the laminar profile make the determination of a critical Reynolds number above which turbulence can be observed a tricky business, as attested by the huge variability of critical numbers that can be found in the literature. The turbulent trajectories above about 1650, and most reference books and textbooks quote numbers in the range of 2000 to 3000[2]. But an interesting feature of turbulence present in pipe flow that is below Reynolds numbers of about 2700. In addition, roughness becomes important in high Reynolds number flows [3]. The study of flow in non-straight pipes dates back to Nikuradse's experiments[4] whose results obtained from artificially roughened pipes, were later arranged in the more well-known form of the Moody Diagram [5] where for laminar flow, the friction factor is usually shown as independent of the roughness. Despite this, several numerical and experimental studies have shown that the contribution of wall shape is not trivial, even in the laminar case. This happens specially when dealing with a wall-shape, rather than just with some random roughness.[6] Many attempts had been made to quantify the effect of roughness on the overlying flow.[7,8,9]. The effect of the roughness shifts the mean velocity profile, downward with respect to a smooth wall and affects the friction factor of forced flow.[10] the change in the wall roughness, imposition of a streamwise pressure gradient, or the presence of a free surface as in open channel flows can impose changes in

boundary conditions and generally it is a nonlinear combination of all the perturbations on the boundary layer [11]. It has been confirmed experimentally that the roughness strip modulated behaviour of the turbulent transport of the Reynolds stresses especially in the region between the two internal layers and more pronounced on the rough surface than flat surface and the turbulent kinetic energy increased in rough surface than smooth surface [12].

Moreover the drag reduction in turbulent flows at low Reynolds numbers associated with the corrugation configurations (such as triangular, trapezoidal and "d-type" square forms) [13]. Experimentally, it was showed that the global friction factor increased in corrugated pipes in compare with that of smooth pipes [14] and spirally corrugated pipes with cavities much larger than the rib height tend to increase the global friction factor in comparison with smooth pipes [15]. Finally, the friction factor increases with Reynolds number and grooves length [16]. This paper focus on the effect of the corrugated shape on the friction factors for turbulent flow in a pipe using computational fluid dynamics and the two-equation turbulence models for numerical simulation.

NOMENCLATURE

U_i	[m/s]	components of the velocity vector,
x_i	[m]	components of the position vector,
t	[s]	Time,
ρ	[kg/m ³]	Fluid density,
P	[N/m ²]	Pressure,
μ	[N.s/m]	dynamic Viscosity,
μ_t	[N.s/m]	Turbulent viscosity,
k	[kg/m-s]	Turbulence kinetic energy,
ε	[kg/m-s]	Turbulence dissipation,
σ_{ij}		Reynolds stress tensor,
v^*	[m/s]	friction velocity
ν	[m ² /s]	kinematic viscosity.
U	[m/s]	velocity
D	[m]	diameter
g	[m/s ²]	acceleration due to gravity.
f	[-]	friction factor,
Re	[-]	Reynolds number and

THE GOVERNING EQUATIONS

The Incompressible and isothermal fluid flow in pipes govern by mass and momentum conservation equations, and in the present work these equations are solved for turbulent flow using k - ε turbulence model,

Conservation of Mass

$$\frac{\partial \rho}{\partial t} + \frac{\partial \rho u_i}{\partial x_i} = 0 \quad (1)$$

Conservation of momentum

$$\rho \frac{\partial U_i}{\partial t} + \rho \frac{\partial U_i U_j}{\partial x_j} = \frac{\partial}{\partial x_j} \left(\mu \left(\frac{\partial U_i}{\partial x_j} + \frac{\partial U_j}{\partial x_i} \right) \right) - \frac{\partial \bar{p}}{\partial x_i} + \rho g_i + S_{ui} \quad (2)$$

By Boussinesq hypothesis

$$-\rho \overline{U_i U_j} = \mu_t \left(\frac{\partial U_i}{\partial x_j} + \frac{\partial U_j}{\partial x_i} \right) - \frac{2}{3} \delta_{ij} \rho k$$

Equation 2 can be rewritten as

$$\rho \left(\frac{\partial U_i}{\partial t} + U_j \frac{\partial U_i}{\partial x_j} \right) = -\frac{\partial P}{\partial x_i} + \frac{\partial}{\partial x_j} \left((\mu + \mu_t) \left(\frac{\partial U_i}{\partial x_j} + \frac{\partial U_j}{\partial x_i} \right) \right) \quad (3)$$

Neglect source term S_{ui} and gravity term ρg_i effect in above equation

Express the above equation in cylinder polar coordinate (2D)

$$\frac{\partial \rho}{\partial t} + \rho \left(\frac{\partial U_r}{\partial r} + \frac{U_r}{r} + \frac{\partial u_z}{\partial z} \right) = 0 \quad (4)$$

Along radial coordinate:

$$\rho \left(U_r \frac{\partial U_r}{\partial r} + U_z \frac{\partial U_r}{\partial z} \right) = -\frac{\partial P}{\partial r} + (\mu + \mu_t) \left(\frac{1}{r} \frac{\partial}{\partial r} \left(r \frac{\partial U_r}{\partial r} \right) - \frac{U_r}{r^2} \right) + (\mu + \mu_t) \left(\frac{\partial^2 U_r}{\partial z^2} + r \frac{\partial^2 U_r}{\partial z \partial r} \right)$$

Along axial coordinate:

$$\rho \left(U_r \frac{\partial U_z}{\partial r} + U_z \frac{\partial U_z}{\partial z} \right) = -\frac{\partial P}{\partial z} + \frac{1}{r} \frac{\partial}{\partial r} \left((\mu + \mu_t) \left(r \frac{\partial U_z}{\partial r} + r \frac{\partial U_r}{\partial z} \right) \right) + (\mu + \mu_t) 2 \left(\frac{\partial^2 U_z}{\partial z^2} \right) \quad (4)$$

Two-equation models (k - ε)

In the two-equation models, two PDEs equations for the turbulent kinetic energy and the turbulent dissipation rate. The turbulent viscosity is expressed as a function of K and ε and equations (8) and (9) are formed.

Turbulence energy equation:

$$\rho \left(\frac{\partial k}{\partial t} + U_j \frac{\partial k}{\partial x_j} \right) = \sigma_{ij} \frac{\partial U_i}{\partial x_j} - \rho \varepsilon + \frac{\partial}{\partial x_j} \left[\left(\mu + \frac{\mu_t}{\sigma_k} \right) \frac{\partial k}{\partial x_j} \right] \quad (5)$$

Turbulence dissipation equation:

$$\rho \left(\frac{\partial \varepsilon}{\partial t} + U_j \frac{\partial \varepsilon}{\partial x_j} \right) = C_{\varepsilon 1} \frac{\varepsilon}{k} \sigma_{ij} \frac{\partial U_i}{\partial x_j} - C_{\varepsilon 2} \frac{\varepsilon^2}{k} + \frac{\partial}{\partial x_j} \left[\left(\mu + \frac{\mu_t}{\sigma_\varepsilon} \right) \frac{\partial \varepsilon}{\partial x_j} \right] \quad (6)$$

Where $C_{\varepsilon 1} = 1.44$, $C_{\varepsilon 2} = 1.92$, $C_{\mu} = 0.09$, $\sigma_k = 1.0$, $\sigma_\varepsilon = 1.3$

and turbulent viscosity $\mu_t = \rho C_{\mu} \frac{k^2}{\varepsilon}$

$$\sigma_{ij} = \left(\frac{\partial U_i}{\partial x_j} + \frac{\partial U_j}{\partial x_i} \right) \quad (7)$$

To solve equations (5) and (9) numerically is complex. The Boussinesq approximation is used to solve the turbulence [17].

$$v^* = C_{\mu}^{0.25} K_p^{0.5} \quad \varepsilon_p = \frac{C_{\mu}^{0.75} K_p^{1.5}}{k y_p} \quad (8)$$

The friction velocity proposed [18] $v^* = \sqrt{\Delta PD / 4\rho L}$ (9)

Friction factors

The following equations can be used to estimate the friction factor

(a) Darcy-Weisbach relation

The pressure drop, ΔP as;

$$\Delta P = f \frac{L}{D} \frac{\rho U^2}{2g} \quad (10)$$

(b) Colebrook -White [18] expression

$$\frac{1}{\sqrt{f}} = -2 \log \left[\frac{c/D}{3.7065} + \frac{2.5226}{Re \sqrt{f}} \right] \quad (11)$$

(c) Romeo et al. Expression[18]:

$$\frac{1}{\sqrt{f}} = -2 \log \left[\frac{c}{3.7065D} - \frac{5.0272}{Re} A \right] \quad (12)$$

Where

$$A = \log \left[\frac{c}{3.706D} - \frac{4.567}{Re} \log \left(\left(\frac{c/D}{7.7918} \right)^{0.9974} + \left(\frac{5.3326}{208.815 + Re} \right)^{0.9345} \right) \right]$$

(d) Blasius correlation that is widely accepts for flow that the Reynolds number less than 10^5 . $f_{smooth} = 0.3162 Re^{-0.25}$

Boundary conditions

The flow is considered to be steady, incompressible and adiabatic. 2D axis metric model is used one of the boundaries is parallel to the flow (axial symmetry boundary condition) and the other is coincides with centreline of the pipe. The velocity along the radial is U_r and along the axial is U_z . The boundaries perpendicular to the flow represent inflow and outflow boundaries. Assuming the flow is fully developed.

The following conditions are assumed

$$\frac{\partial U_r}{\partial z} = 0 \quad \frac{\partial U_z}{\partial z} = 0 \quad \frac{\partial k}{\partial z} = 0 \quad \frac{\partial \epsilon}{\partial z} = 0 \quad (13)$$

Assuming there is no slip along the wall.

$$U_r(0,z) = 0 \quad \text{and} \quad U_r(c,z) = U_z(c,z) = 0 \quad (14)$$

where c is the groove height . the velocity of the flow at the centre is the maximum flow.

$$\text{i.e. } U_r(c,z) = U_z(c,z) = U_{max} \quad (15)$$

For the pressure, the conditions at the inflow and outflow pressures along the axial length L are considered as following.

$$P(x_1,L) = P(x_1,0) - \beta \Delta x_2 \quad (16)$$

Where β is the pressure gradient and $P(x_1,0)$ is the inflow pressure and $P(x_1,L)$ is the outflow pressure. The term $-\beta \Delta x_2$ represents the pressure drop along the direction of flow.

$$\frac{\partial P}{\partial r} = 0 \quad (17)$$

Geometrical modelling

Five different configurations were assumed for the corrugate pipe, involving grooves height and length. Figure below shows the representative dimensions of the corrugated pipe, where a represents the grooves spacing, b is the groove length, c is the groove height, s is the pitch between two consecutive grooves and D is the pipe inner diameter.

Consider Length, $L = (a+b)$ if $a/D = xa$ and $b/D = xb$

Equation (18) become

$$V^* = \sqrt{\Delta P / 4\rho S} \quad (18)$$

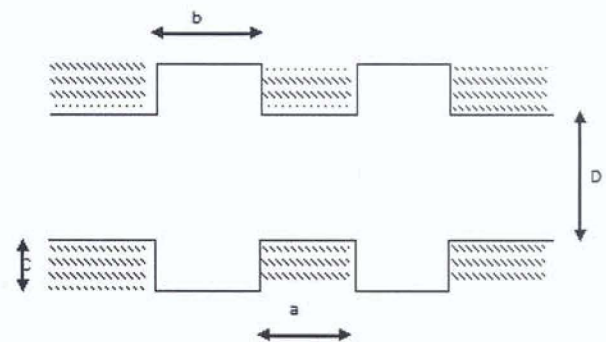


Figure1. The main dimension of the corrugated pipe

Configuration	a/D	b/D	c/D
1	0.11	0.05	0.03
2	0.11	0.03	0.03
3	0.11	0.04	0.03
4	0.11	0.04	0.04
5	0.15	0.04	0.04

Table.1: Numerical values of the main dimensions shown in Fig. 3.1, for the five geometric configurations assumed [15]

NUMERICAL SIMULATION: RESULT AND DISCUSSION

Water is considered as the fluid properties with assumed density $\rho = 1000 \text{ kg/m}^3$, dynamic viscosity, $\mu = 1 \times 10^{-3}$ and Kinematic viscosity $\nu = 1 \times 10^{-6} \text{ m}^2/\text{s}$. For easy simulation the pressure difference is assumed to be 1000 N/m^2 and diameter of the pipe assumed to be 100 mm . MATLAB language was used to solve the problems to return the friction factors for the Reynolds number $10000, 20000, 30000, 40000$ and 50000 . These Reynolds numbers were used to compute the corresponded friction factor using Colebrook, Romel expressions and Blasius correlation. The dimensions were rated with the diameter of the pipe.

Result

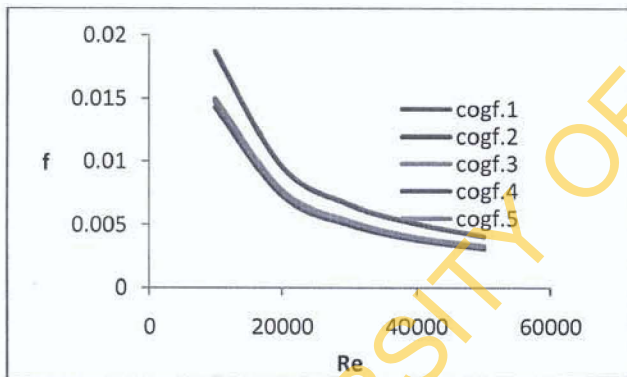


Figure 2: The friction factors at different Reynolds number for the five configurations

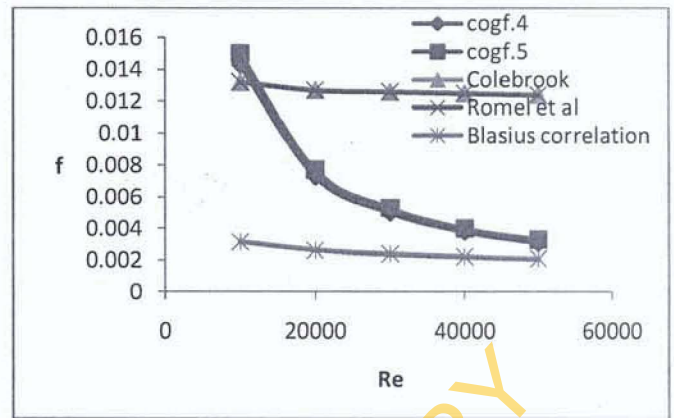


Figure3: The comparison between present work, colebrook, Romel, and Blasius correlation for configurations 1 and 3

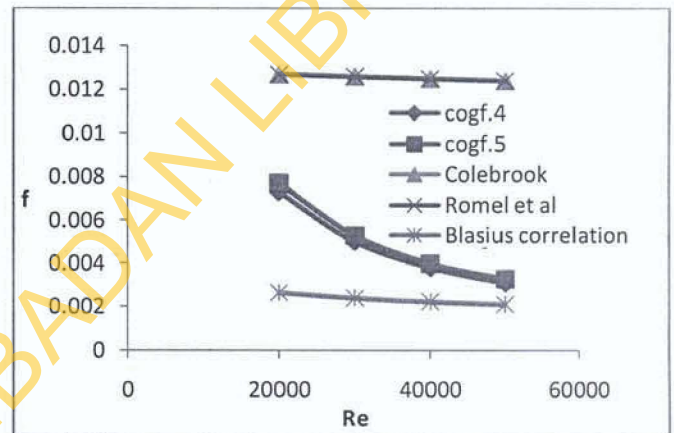


Figure4: The comparison between present work Colebrook, Romel and Blasius for configurations 4 and 5

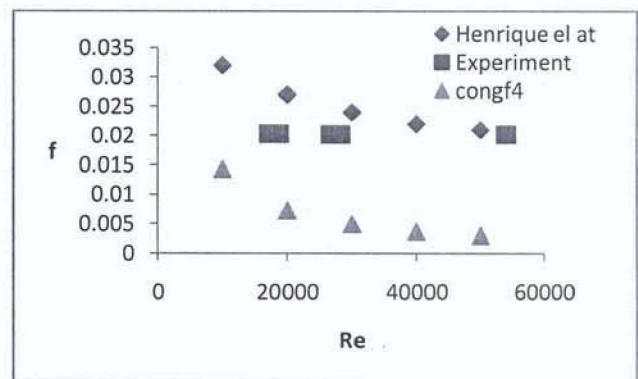


Figure5: The comparison between present work Henrique el at results and experimental results (Morales el at) for configurations 4.

Discussions

The grove is constant in all configurations which represent the roughness height of the Colebrook White and Romel et al

equations at 3% of the diameter of the pipe. The groove height is 1.1% of the diameter for configurations 1 to 4 but 1.5% for configuration 5. From the figure 2, the friction factor reduced as the Reynolds number increased. The effects of the configurations on the friction factor were pronounced in configuration 1 than others. The change in groove length dimension was much in configuration 1. The groove length was 5% while configuration 2 was 3% and configuration 3, 4 and 5 were 4%. As groove spacing increased, the friction factors increased. This agreed with Henrique et al report and shown that the groove length affects the friction factor flow. i.e. the groove length contributes to turbulence of the flow. The effect of the corrugated surface on the friction factor is very low even at high Reynolds numbers. The friction factor at this configuration is closed to corresponding Reynolds numbers using the Colebrook White and Romel et al formulae and the smooth formula of the Blasius correlation is differed from others. In the figure 3 and 4 shown the friction factor always greater than the smooth flow and the Colebrook White and Romel values at Reynolds number low than 20000. The figure 5 shown the similarity between the present work with Henrique et al results and Morales et al experimental results for configuration 4

Conclusion

It can be concluded that the groove length and spacing contribute to the loss of pressure flow in the pipe. From the discussion with increase in the groove lengths and spacing, increase the friction factor. The increase in the friction factor is as a result of a momentum transfer enhancement between the confined recirculation in the groove which can cause fluctuation of the velocity near the corrugated. The friction factor does not depend only on the roughness height alone but also on the thickness and spacing of the roughness. The equations depend lonely on the roughness height cannot give accurate friction factor in the pipes..

REFERENCES

- [1] Prandtl, L., Tietjens, O.G., 1883, 'Applied Hydro- and Aeromechanics' (Dover Publications, New York, 1934). O. Reynolds, Phil. Trans. Roy. Soc. (London) 174, 935.
- [2] Darbyshire, A.G., and Mullin, T., 1995, Journal of Fluid Mechanics volume 289, page 83.
- [3] Wygnanski I.J., F.H. Champagne F.H., 1973, ' Journal of Fluid Mechanics volume 59, page 281.
- [4] Wygnanski, I.J., Sokolov, M., Friedman, D., 1975, Journal of Fluid Mechanics Volume 69, page 283.
- [5] Nikuradse, J., 1933, Stormungsgesetz in rauhren rohren, vDI Forschungshefte 361 (English translation: Laws of flow in rough pipes.). NACA Technical Memorandum 1292, National Advisory Commission for Aeronautics, Washington, DC, USA.
- [6] Moody, L. F., 1944, 'Friction factors for pipe flow' Trans. ASME, 66(8), November, pp. 97-107.
- [7] Lessen, M., and Huang, P., 1976, 'Poiseuille flow in a pipe with axially symmetric wavy walls', The Physics of Fluids, 19(7), July, pp. 945-950.
- [8] Inaba, T., Ohnishi, H., Miyake, Y., and Murata, S., 1979, 'Laminar flow in a corrugated pipe' Bulletin of the JSME, 22(171), September, pp. 1198-1204.
- [9] Blackburn, H. M., Ooi, A., and Chong, M. S., 2007, 'The effect of corrugation height on flow in a wavy-walled pipe, 16th Australasian Fluid Mechanics Conference, A. Editor and B. Editor, eds., pp. 559-564.
- [10] Rotta, J.C., 1962, 'Turbulent boundary layer incompressible flow', Progress in Aeronautical Sciences, vol. 2. Pergamon press, Oxford
- [11] Perry, A.E., Schofield, W.H., Joubert, P.N., 1969, 'Rough wall turbulent boundary layers' Journal of Fluid Mechanics 37, 383-413.
- [12] Witz, J. A., Ridolfi, M. V., and Hall, G. A., 2004, 'Offshore LNG transfer - a new flexible cryogenic hose for dynamic service', Offshore Technology Conference (Witz et al, 2004).
- [13] Clauser, F.H., 1956, 'The turbulent boundary layer' Advances in Applied Mechanics, 4: 1-51
- [14] Oyewola Olanrewaju M., 2007, 'Measurements of higher-order turbulent statistics in a turbulent boundary layer subjected to a short roughness' striphermal science, Volume 11, No. 4, pp. 41-48.
- [15] Chen, J.J., Leung, Y.C., Ko, N.W., 1986, 'Drag Reduction in a Longitudinally Grooved Flow Channel', Industrial and Engineering Chemistry Fundamentals, Vol. 25, pp. 741-745.
- [16] Morales, R.E.M., Franco, A.T., Junqueira, S.L.M., Erthal, R.H., 2007, "Experimental Analysis of Turbulent Flow in Flexible Pipes" Technical Report - UTFPR/CENPES-PETROBRAS, Curitiba,
- [17] Dong, Y., Huixiong, L., Tingkuan, C., 2001, "Pressure Drop, Heat transfer and Performance of Single-Phase Turbulent Flow in Spirally Corrugated Tubes, Experimental Thermal and Fluid Science, Vol. 24, pp. 131-138.
- [18] Henrique S. de Azevedo, Rigoberto E. M. Morales, Admilson T. Franco, Silvio L. M. Junqueira, Raul H. Erthal, 2008, 'Numerical Simulation of turbulent flow in corrugated pipes' proceedings of ENCIT 2008 12th Brazilian Congress of Thermal Engineering and Sciences by ABCM November 10-14, 2008, Belo Horizonte.
- [19] Silberman, E., 1980, 'Turbulence in Helically Corrugated Pipe Flow', Journal of the Hydraulics Division, Proceeding of the American Society of Civil Engineers, Vol. 106, N° EM4, pp. 699-717.